Formation of Brown Lines in Paper: Characterization of Cellulose Degradation at the Wet-Dry Interface

Zied Souguir, Anne-Laurence Dupont, E René de La Rie

Formation of Brown Lines in Paper: Characterization of Cellulose Degradation at the Wet−Dry Interface

Zied Souguir and Anne-Laurence Dupont*

Centre de Recherche sur la Conservation des Collections, Muséum National d'Histoire Naturelle, CNRS-UMR 7188, 36 rue Geoffroy-Saint-Hilaire, 7005 Paris, France

E. René de la Rie†

National Gallery of Art, 401 Constitution Avenue NW, Washington, DC 20565

Received June 2, 2008; Revised Manuscript Received July 15, 2008

Brown lines were generated at the wet−dry interface on Whatman paper No. 1 by suspending the sheet vertically in deionized water. Formic acid and acetic acid were quantified in three areas of the paper defined by the wet−dry boundary (above, below, and at the tideline) using capillary zone electrophoresis with indirect UV detection. Their concentration increased upon accelerated aging of the paper and was highest in the tideline. The hydroperoxides have been quantified using reverse phase high performance liquid chromatography with UV detection based on the determination of triphenylphosphine oxide produced from the reaction with triphenylphosphine, and their highest concentration was found in the tideline as well. For the first time, it was shown that various types of hydroperoxides were present, water-soluble and non-water-soluble, most probably in part hydroperoxide functionalized cellulose. After accelerated aging, a significant increase in hydroperoxide concentration was found in all the paper areas. The molar masses of cellulose determined using size-exclusion chromatography with multiangle light scattering detection showed that, upon aging, cellulose degraded significantly more in the tideline area than in the other areas of the paper. The area below the tideline was more degraded than the area above. A kinetic study of the degradation of cellulose allowed determining the constants for glycosidic bond breaking in each of the areas of the paper.

1. Introduction

Formation of brown lines at the wet−dry interface in cellulosic materials has been described in several publications, some of which date from as far back as 1930.[1−11] The formation of these so-called "tidelines" has been described for cellulosic textiles as well as for sheets of paper. Despite various research efforts, the mechanism of brown line formation is not clearly understood.

A tideline can be produced by suspending a strip of paper vertically with the lower end immersed in water. The water will rise in the strip through capillary action until equilibrium is reached, where the capillary rise is offset by evaporation. Within a few hours, a brown line forms at the wet−dry interface. Fluorescence can be detected in the tideline area even earlier.[2,9,11,12] While the discoloration and fluorescence appear to be caused largely by water-soluble products and can therefore be removed, it has been evidenced that cellulose is degraded in the tideline area, as indicated by the formation of insoluble carboxylic acid group containing species (methylene blue absorption), by a decrease in degree of polymerization (cuprammonium fluidity[4]) and by an increased hydroperoxides concentration.[11]

Although migration of colored water-soluble products to the tideline area might be suspected, and this may certainly occur in aged discolored papers, brown lines can be generated with distilled water in pure cellulose paper such as Whatman paper No. 1. If such sheets are prewashed, the tideline phenomenon is reduced, but after storage for a few weeks of these washed sheets, brown lines similar to those occurring in unwashed paper are produced.[11] It appears, therefore, that active species are formed in the sheets within weeks, which migrate to the tideline area and cause the degradation. The degradation appears to be oxidative in nature, but the exact mechanism is still largely unknown. Possibly, hydrogen peroxide, water-soluble alkyl hydroperoxides and free radical species, such as peroxy, alkoxy, and hydroxyl radicals, present in the sheet, accumulate in the tideline area, where they meet with oxygen and rapidly multiply as a result of free radical chain reactions, leading to colored and other degradation products. A better understanding of this phenomenon is of relevance to the conservation, storage, and the treatment of cultural objects made of paper. Local wet treatments in particular may involve the formation of tidelines. Many discoloration phenomena occurring in paper objects, including foxing stains, which involve severe oxidation of cellulose,[13] may be caused by reactions at the wet−dry interface.[14−16] An understanding of the process is also of general relevance to the understanding of cellulose degradation chemistry.

In this work, the type of degradation incurred during tideline formation was explored. Chemical species present at the tideline were analyzed and, for the first time, precisely quantified, focusing on small organic acids using capillary zone electrophoresis (CZE) and on hydroperoxides. The latter were determined by quantifying the amount of triphenylphosphine oxide (TPPO) produced by their reaction with triphenylphosphine (TPP), using reverse phase high performance liquid chromatography (RPLC). The macromolecular modification of cellulose was investigated by measuring the molar masses (M_r) using size-exclusion chromatography with multiangle light scattering

* To whom correspondence should be addressed. Tel.: +33 140795307. Fax: +33 140795312. E-mail: aldupont@mnhn.fr.

† Mailing address: 2000B South Club Drive, Landover, MD 20785.

10.1021/bm8006067 CCC: $40.75
Published on Web 08/21/2008

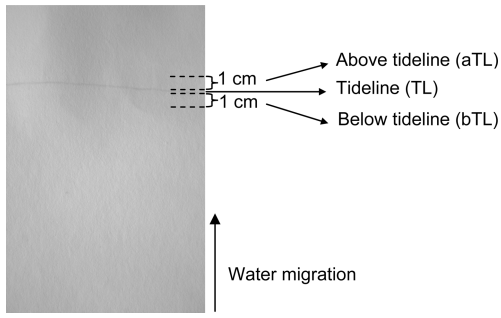

Figure 1. Photograph of Whatman paper No. 1 with a tideline showing the areas as defined for the chemical analyses.

detection (SEC/MALS). The evolution of the macromolecular features during the accelerated aging of the samples made possible a kinetic study of the degradation of cellulose at the wet−dry interface.

2. Experimental Section

2.1. Materials and Chemicals. Whatman paper No. 1, composed of 100% cotton cellulose fibers, was used. TPP (ReagentPlus, 99%) and potassium formate (99%) were purchased from Sigma-Aldrich. TPPO, sodium acetate (>99%), *N*,*N*-dimethylacetamide, and lithium chloride anhydrous were from Fluka.

2.2. Experimental Setup. Several sheets of Whatman paper No. 1 (15 cm × 28 cm) were suspended vertically, 2 cm deep in deionized water at ∼4−5 cm intervals. The experiment was carried out in the dark in a climatized room at 23 °C, 50% rH, and lasted 16 h. The wet−dry interface stabilized around 20−21 cm from the bottom of the sheet. The formation of the brown line started after a few hours. The sheets were then left to dry. Three areas in the paper were analyzed after the tideline experiment: the tideline, the area above the tideline, and the area below the tideline (abbreviated TL, aTL, and bTL, respectively; Figure 1). The brown line was cut from the paper as close on each side of the brown boundaries as possible. The areas above and below were cut on the whole width of the paper after the brown line was cut-out and were 1 cm wide, approximately.

2.3. Organic Acids Analysis by CZE. *2.3.1. Sample Preparation.* A total of 60 mg of paper cut in small pieces were immersed in 2 mL of deionized water at ambient temperature for 1 h. The aqueous extract was filtered on a PTFE filter (0.45 μm; Millipore) before the analysis.

2.3.2. Analysis Conditions. The CZE equipment was a P/ACE MDQ equipped with a PDA detector (Beckman Coulter). The system operation, data acquisition, calibration, and quantitation were performed using 32 Karat 5.0 software (Beckman Coulter). The compounds were identified according to their migration time t_m compared to known standard compounds. When attribution was uncertain, spiking the sample solution with the suspected standard compound was done for confirmation.

The analysis of organic acids was performed using a method previously developed.[17] Indirect UV detection at 350 nm was used with the reference at 200 nm and a bandwidth of 20 nm. Data collection rate was set to 4 Hz. A bare-fused silica capillary with 75 μm internal diameter (ID; Beckman Coulter) was cut to a total length of 60 cm (effective length to the detection window L_{eff} = 50.2 cm). Prior to injection, the capillary was rinsed 1 min with NaOH 0.1 M followed by deionized water for 1.5 min. The capillary was then conditioned during 1 min with the run buffer. The buffer was prepared with 2,6-pyridinedicarboxylic acid (PDC; 5 mM) as background electrolyte (BGE) and cetyltrimethylammonium bromide (CTAB; 0.5 mM), pH 5.6 (adjusted with NaOH 1 M). The injection was made in hydrodynamic mode by applying a pressure of 0.7 psi during 4.5 s. A separation voltage of −25 kV was applied to the anodic end. The resulting current was 15 μA. The run temperature was 25 °C. After each analysis the capillary was rinsed during 2 min with deionized water.

2.3.3. Method Validation. Sensitivity of the method was evaluated with the limit of detection (LOD) calculated as three times the signal-to-noise ratio, and with the limit of quantitation (LOQ) calculated as 3.33 × LOD.[18] The linearity of the response was established for each model analyte by building calibration curves with 6 to 7 concentration levels using three individual solutions for each level. Each calibration point corresponded to the average of five injections. Calibration curves for both acids were performed over the concentration range 5−200 mg L^{-1}.

2.4. Hydroperoxides Analyses by RPLC. *2.4.1. Sample Preparation.* The reagent was a solution of TPP in acetonitrile (0.136 g L^{-1}). Two types of samples were prepared. The first type allowed measuring water-soluble hydroperoxides only. Approximately 200 mg of paper were immersed in 2 mL of deionized water for 48 h at ambient temperature. The filtered sample solution (500 μL) was then mixed with the TPP reagent solution (500 μL). The second type of sample allowed measuring the total hydroperoxide content (water-soluble and non-water-soluble). Approximately 200 mg of paper were immersed in 3 mL of TPP reagent solution previously diluted with deionized water (1:1). The reaction was allowed to proceed for 2 h. Samples were filtered through PTFE filters (0.45 μm; Millipore) prior to analysis.

2.4.2. Analysis Conditions. A dual gradient high pressure analytical pump System Gold model 126 (Beckman Coulter), manual injector (7725i, Rheodyne), and diode array detector (DAD) model 168 (Beckman Coulter) were part of the chromatographic setup. The separation was carried out on a C18 Sinergi Hydro-RP column (4 μm particle-diameter, L × D 150 mm × 2 mm, Phenomenex), preceded by a guard column (SecurityGuard, Phenomenex). The column compartment was thermostatted at 25 °C. The mobile phase consisted of a mixture of water (solvent A) and acetonitrile (solvent B). The linear gradient used was the following: 0−0.5 min, 0% B; 0.5−5.5 min, 0−100% linear B; 5.5−20.5 min, 100% B. The system was equilibrated with 100% water during 15 min before each run. The flow rate was 0.3 mL min^{-1}, and the injection volume was 20 μL. The full DAD UV scan was made over the entire range of 160−280 nm, and the detection of the peaks was done at 225 nm. The system operation, data acquisition, calibration, and quantitation were performed using 32 Karat 5.0 software (Beckman Coulter).

2.4.3. Method Validation. LOD and LOQ were calculated as described in Section 2.3.3. The linearity of the response was established by building calibration curves with five concentration levels using three individual solutions for each level. Each calibration point corresponded to three injections. The calibration curve for TPPO was done over the concentration range 4.7 × 10^{-6} to 3 × 10^{-4} mol L^{-1}.

2.5. M_r Determination by SEC. The average molar mass of cellulose was determined using SEC-MALS. An isocratic HPLC pump 515 (Waters) and autosampler ACC-3000T (Dionex) were part of the chromatographic setup. The MALS detector was a Dawn EOS (Wyatt Technologies), and the differential refractive index (DRI) detector was a 2414 (Waters). The laser source of the MALS has a nominal power of 25 mW and operates at 690 nm, the LED of the DRI emits at 880 nm. The interdetector delay volume was determined as 0.22 mL. The constants of the instruments as experimentally determined were 7.187 × 10^{-6} for the MALS and 2.417 × 10^{-5} V^{-1} for the DRI.

The separation was carried out on a set of three polystyrene divinyl benzene (PSDVB) columns Phenogel Linear(2) (5 μm particle-diameter mixed bed pores columns, L × D 300 mm × 4.6 mm, Phenomenex) preceded by a guard column Phenogel (5 μm, L × D 30 mm × 4.6 mm, Phenomenex). The columns compartment (Interchim, model 102) and the MALS detector were thermostatted at 60 °C and the DRI was set to 55 °C. The mobile phase, *N*,*N*-dimethylacetamide with 0.5% lithium chloride (wt/vol; LiCl/DMAc), was filtered through 0.5 μm pore Millex LCR filters (Millipore) prior to use. The system was operated at a flow rate of 0.4 mL min^{-1} with an injection volume of 100 μL, and the run time was 30 min. The dissolution of the paper samples

prior to the analysis was carried out in 8% LiCl/DMAc, according to a procedure detailed in a previous publication.[19] The data acquisition was carried out with ASTRA software version 5.3.1.5 (Wyatt Technologies) in 0.5 s intervals. The value of d*n*/d*c* of cellulose in 0.5% LiCl/DMAc at 55 °C and 880 nm was experimentally determined online, in chromatographic mode, assuming 100% sample recovery from the columns, as 0.140 mL g^{-1}. A 5% mass loss was estimated (and validated through the calculated sample mass by ASTRA software) as the maximum possible loss originating from the sample activation phase prior to dissolution, which involves several filtering steps[19] and was applied to the value of the sample injected mass. The d*n*/d*c* of cellulose in LiCl/DMAc is particularly difficult to establish, and a wide array of values can be found in the literature.[20] The value determined here differs from the value previously determined offline (without the columns)[20] but is consistent with the value reported by Röhrling et al.[21] The value determined in chromatographic mode was preferred in the present case with regard to the conformational behavior of cellulose in the solvent LiCl/DMAc, which is most likely to be that of a polyelectrolyte complex.[22] Each sample solution was run three times nonconsecutively. The repeatability of the method as previously determined was RSD % = 2.5 on M_w for three separate cellulose samples analyzed two to three times nonconsecutively.

2.6. Accelerated Aging. The accelerated aging of the papers was carried out following the ASTM standard method D6819−02e02.[23] The entire sheet of paper with the brown line (4 g) was placed inside a 150 mL glass tube (Wheaton), which was tightly closed with a screw-cap specified as heat-resistant (in the range −196 to +260 °C) and a Teflon/silicon liner. The tubes were placed in a dry heat oven (Memmert) at 100 °C. The aging lasted from 1 to 120 h. Before insertion in the glass tube, the paper was preconditioned to 23 °C and 50% rH in a climate room to attain the same moisture content of the samples, that is, 5 wt %/wt, as measured using TAPPI T 412 om-94[24] (the glass tubes and the caps were also kept in the climate room). In this type of accelerated aging, the relative humidity inside the tube, which is regulated by the moisture content of the paper, was estimated to be approximately 45−55%. It is indeed crucial to keep reproducible moisture contents during the aging, as moisture takes an active role in the chemical degradation of cellulose at high temperatures through hydrolysis[25,26] and, as it has been shown, different levels of humidity have very large effects on the aging of paper.[27] Once out of the oven, the glass tubes were left to cool before opening and the paper samples were subsequently reconditioned during 24 h to 23 °C and 50% rH before analysis.

3. Results and Discussion

3.1. Organic Acids Quantitation. Determination coefficients for the calibration curves of formic acid and acetic acid were 0.9993 and 0.9999, respectively, indicating a good precision of the method. LODs of 4.77 μmol L^{-1} and 8.68 μmol L^{-1} and LOQs of 16.06 μmol L^{-1} and 28.56 μmol L^{-1} were determined for formic acid and acetic acid, respectively, indicating a good sensitivity of the method.

The major peaks identified on the electropherograms of aqueous extract of the tideline were formate and acetate (Figure 2). A minor peak was also present, which could not be identified, as no match was found among the standard organic acids tested (glycolic, succinic, lactic, hexanoic, peroxyacetic). Two large unresolved peaks eluted before 2.5 min and were attributed to small inorganic anions. They were identified separately (by CZE) as nitrate, chloride, and sulfate. These anions are initially present in the paper. The concentrations of formic acid and acetic acid found in the tideline, above the tideline, and below the tideline for the samples unaged and aged 48 and 120 h are reported in Table 1. The concentrations generally increased after accelerated aging in the three areas in various proportions. This result was expected, as it had been previously shown that organic

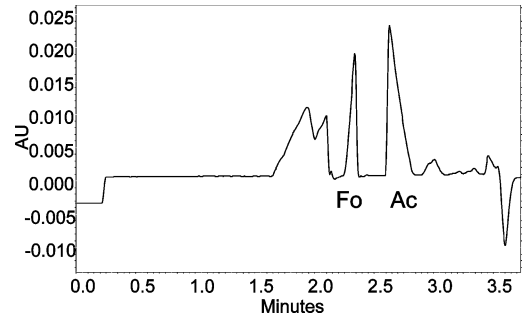

Figure 2. Electropherogram of an aqueous extract of tideline showing formic acid (Fo) and acetic acid (Ac). Capillary 75 μm × 60 cm (L_{eff} = 50.2 cm). BGE PDC 5 mM; CTAB 0.5 mM, pH 5.6; hydrodynamic injection 0.7 psi, 4.5 s; applied potential −25 kV; temperature 25 °C; detection: signal = 350 nm, reference = 200 nm.

Table 1. Amount of Formic Acid (Fo) and Acetic Acid (Ac) in the Tideline (TL), above the Tideline (aTL), and below the Tideline (bTL)[a]

	0 h (mmol g^{-1}_{paper})		48 h (mmol g^{-1}_{paper})		120 h (mmol g^{-1}_{paper})	
	[Fo]	[Ac]	[Fo]	[Ac]	[Fo]	[Ac]
aTL	NQ[b]	NQ	0.2478	0.1417	0.2378	1.59
TL	147.4	223	233	213	264.3	497.3
bTL	NQ	NQ	0.1657	0.063	0.3926	0.5067

[a] Before and after accelerated aging in closed vessels at 100 °C for 48 and 120 h. [b] NQ: not quantifiable (below LOQ).

Table 2. Amount of Formic Acid (Fo) and Acetic Acid (Ac) in the Paper[a]

	[Fo] (mmol g^{-1}_{paper})	[Ac] (mmol g^{-1}_{paper})
TL1	147.6	247
TL2	67.3	41.1
TL3	44.1	3.5

[a] In the first tideline (TL1) and in two subsequent tidelines (TL2 and TL3) produced successively with no lag time and on the same sheet of paper.

acid concentrations in paper increase with aging. These two acids have been pointed out as potential indicators of paper degradation.[17] More noteworthy is the fact that the concentration of the two acids was higher in the tideline than in the other areas both before and after aging: 300 to 2000 times higher. Before aging, acids were nearly absent above and below the tideline (not quantifiable). After aging, the concentrations were generally lower in the area below than above the tideline. This result could imply that acids initially present in the paper are concentrating at the wet−dry boundary of the paper upon migration of the water due to capillary rise. To investigate this point, an experiment was carried out in which tidelines were formed three times consecutively on the same sheet of paper. The results showed that if the first tideline contained the highest concentration of acids, measurable amounts were still found in the consecutive tidelines, indicating a rapid reformation of the acids during the tideline experiment (Table 2).

3.2. Hydroperoxide Quantitation. There is a number of methods available for quantitative determination of hydroperoxides.[28] Most of these methods are generic chemical methods that rely on redox reactions. The iodometric assay method based on the oxidation of sodium or potassium iodide followed by the spectrophotometric determination of the I^{3-} chromophore is most commonly used.[29] Another widespread method is based on the formation of complexes of ferric ions by the oxidation of ferrous ions. One method proposes the spectrophotometric determination of these complexes upon reaction in an acidic

Scheme 1. Reduction of a Hydroperoxide by TPP To Form TPPO and an Alcohol

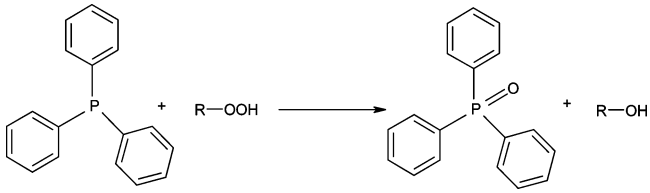

medium containing the dye xylenol orange.[30] The main limitation of these assays is the possible interference from minor compounds other than hydroperoxides as well as their lack of specificity toward other oxidative species. Moreover, a total absence of oxygen and light has to be achieved during the reaction, which is also a source of error.[31] For these reasons, the method that was chosen in this work for the analysis of hydroperoxides was one based on their reduction with TPP[32] (Scheme 1). The reduction of hydroperoxides by trisubstituted phosphines has been shown to be highly specific.[33,34] The TPPO produced can be quantified using RPLC.[35]

3.2.1. RPLC Method Development and Validation. TPPO and TPP are fully resolved on the chromatograms, with $t_R = 10.85$ ($\pm$0.21) min and $t_R = 14.80$ ($\pm$0.20) min, respectively. The calibration curve (Figure 3), which plots peak area as a function of concentration for TPPO, indicates a good linear regression ($R^2 = 0.998$). The method shows high sensitivity as well with LOD = 1.97 ($\pm$ 0.06) μmol L^{-1} and LOQ = 6.56 ($\pm$ 0.20) μmol L^{-1}.

The stability of TPP and the optimal reaction time were evaluated by measuring the production of TPPO from the reaction of TPP to a known concentration of H_2O_2 (=4.50 ($\pm$ 0.30) $\times$ 10^{-4} mol L^{-1}). Figure 4 shows that after 2 h the reaction was complete with matching TPPO and H_2O_2 concentrations.

3.2.2. Hydroperoxides in Unaged Paper. Figure 5 shows the concentration of total hydroperoxides (from the reaction of TPP directly with paper) and the portion of water-soluble hydroperoxides (from the reaction of TPP with aqueous extracts of paper) in the different areas of the paper. The highest concentrations of both types of hydroperoxides were found in the tideline (about six times higher than in the other areas). The amount of total hydroperoxides was larger than that of water-soluble ones

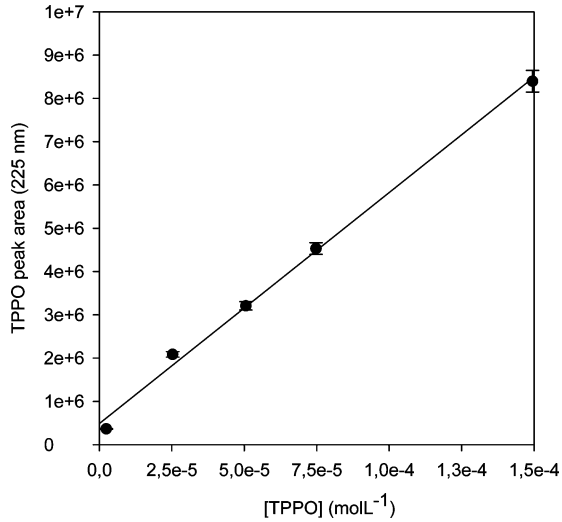

Figure 3. Calibration curve for the quantitation of TPPO (peak areas are measured at 225 nm).

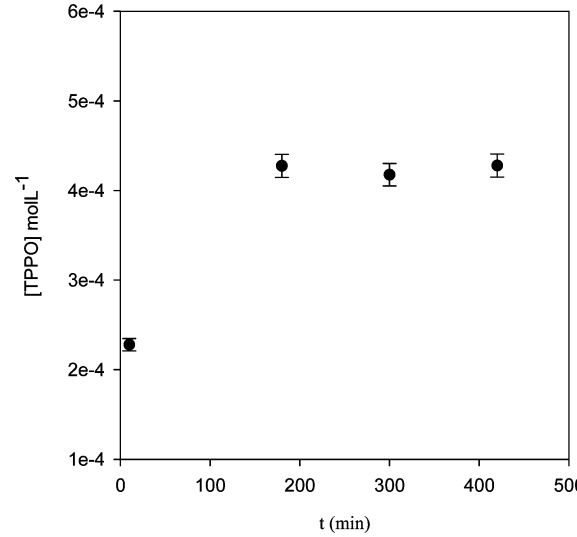

Figure 4. Monitoring of the reaction time of H_2O_2 with TPP.

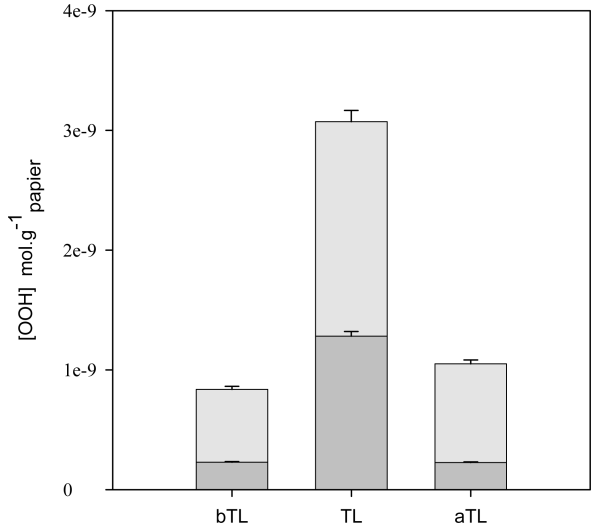

Figure 5. Quantitation of water-soluble hydroperoxides (dark gray) and total hydroperoxides (total of light and dark gray) in the different areas of the paper.

in all the areas of the paper (2.4−4.7 times). This result indicates that the hydroperoxides formed are free hydroperoxides (water-soluble and non-water-soluble) as well as hydroperoxide functionalized cellulose.

3.2.3. Hydroperoxides in Aged Paper. No water-soluble hydroperoxides were found in the aqueous extracts of any of the areas of the aged paper. This could be due to their decomposition at high temperature during the aging process or to their consumption by reactions taking place during aging. The concentration of hydroperoxides in the three areas in the unaged paper and papers aged 48 and 120 h was measured (Figure 6). In all the areas, the hydroperoxide concentration was higher after aging than before, with higher values after 48 h than after 120 h. However, in the aged papers, the difference in hydroperoxide concentration among the areas was not as large as in the unaged paper.

To obtain more precise information on the kinetics of production of hydroperoxides during aging, the total hydroperoxide concentration in the tideline was also determined after accelerated aging of 1, 2, 3, 4, and 5 h (Figure 7). The concentration of hydroperoxides increased with time and then declined, with a maximum observed after 3 h. The curve is

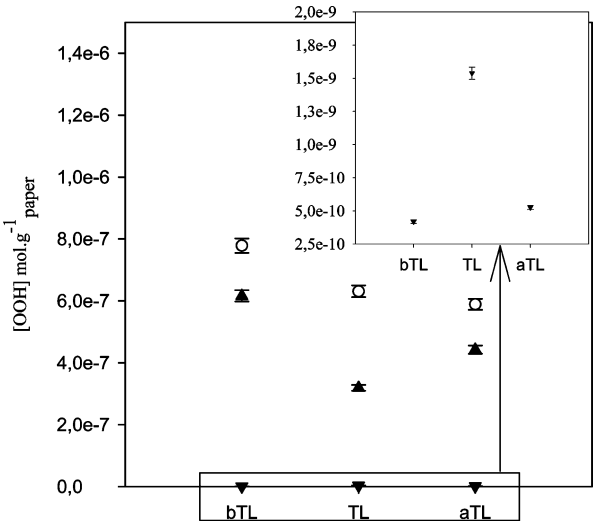

Figure 6. Quantitation of total hydroperoxide concentration in the different areas in paper aged at 100 °C in closed vessel for 48 h (○) and 120 h (▲). Inset: zoom of the unaged samples (▼).

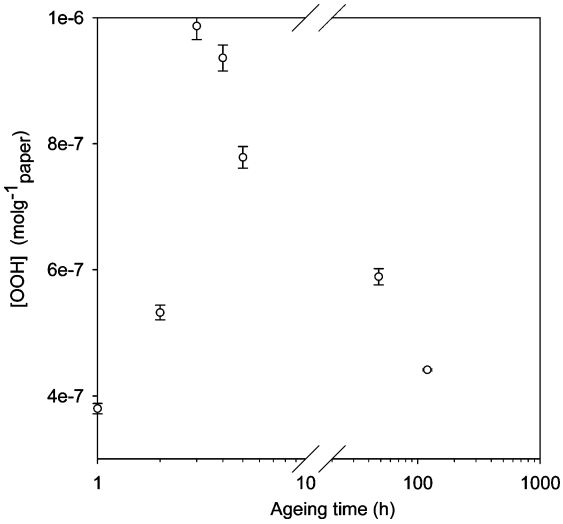

Figure 7. Quantitation of total hydroperoxide concentration in the tideline area upon 1, 2, 3, 4, 5, 48, and 120 h of aging at 100 °C in closed vessel ($[OOH]_{t0} = 3.07 \times 10^{-9}$ mol $g^{-1}{}_{paper}$).

characteristic of the evolution and subsequent consumption of hydroperoxides in materials during autoxidative degradation and confirmed the high reactivity and rapid decomposition of these compounds after their formation.[36]

3.3. M_r Averages and Molar Mass Distribution of Cellulose. Table 3 gathers M_r averages for the areas above, below, and at the tideline in unaged samples, samples aged 48 and 120 h, as well as for reference Whatman paper No. 1. Before aging, the weight average molar mass (M_w) of cellulose in the area above the tideline was 5.71×10^5 (±1.1%) g mol^{-1}, which is similar to that of the reference sample (5.62×10^5 (±2.1%) g mol^{-1}). Among the three areas, a very slight tendency toward lower M_r averages of cellulose in the tideline was noted. Already after 48 h of aging, the M_r averages in all three areas were clearly lower than those in the unaged paper. In the area above the tideline, the aging induced a decrease in M_w of 13.2% after 48 h and 29.1% after 120 h. These M_w values were found to be similar to those of the reference aged in the same conditions, within the RSD%, which showed that the area above the tideline was not affected during aging by volatiles from the more degraded tideline area, thereby validating the accelerated aging protocol. More notably, results showed a considerably higher degradation (lower M_r averages) upon aging in the tideline than in the areas above and below (Table 3). This difference in degradation among the three areas became more noticeable at the longest aging time. It was also noted that the area below the tideline degraded faster than the area above. While the drop in M_w of cellulose for the area above the tideline was 29.1% after 120 h, it was 45.6% at the tideline and 38.8% for the area below. The molar mass distribution (MMD) of cellulose as a function of aging for each area is represented in Figure 8.

3.4. Kinetics of the Degradation of Cellulose. Degradation of cellulose from aging, accelerated by the effects of heat and humidity, is described in the literature as a process governed by random scissions of the polymer chains due to acid-catalyzed hydrolysis.[37−39] The kinetic model for degradation of linear polymer molecules developed by Ekamstam in 1936[40] based on first order kinetics is usually applied to explain the degradation of cellulose under a variety of different conditions (eq 1).

$$\frac{1}{M_t} - \frac{1}{M_{t_0}} = k' t \tag{1}$$

With polydispersity increasing slightly with aging time (Table 3), the number average molar mass M_n is to be used preferably over M_w in eq 1.[41] The slope k' in the plot ($1/M_{nt} - 1/M_{nt0}$) as a function of time t is the reaction rate constant. According to this model, the relationship between ($1/M_{nt} - 1/M_{nt0}$) and aging time t should be linear.[39,42] However, deviation from linearity has been experimentally observed.[43]

With $k' = k/M_o$, where M_o is the molar mass of anhydroglucose, the repeating unit of cellulose (162 g mol^{-1}), the rate constant k of glycosidic bond breaking can be calculated.

Figure 9 shows the plot of the reciprocal of the degree of polymerization ($1/DP_{nt} - 1/DP_{nt0}$) versus aging time (h) for each area of the paper, with $DP_n = M_n/M_o$. The average slopes yielded the constants for glycosidic bond breaking, with $k_{aTL} = 1.67 \times 10^{-6}$ h^{-1} ($R^2 = 0.9997$), $k_{TL} = 3.47 \times 10^{-6}$ h^{-1} ($R^2 = 0.998$) and $k_{bTL} = 2.67 \times 10^{-6}$ h^{-1} ($R^2 = 0.994$). The values are of the same order of magnitude as those determined for cotton linters aged under slightly different conditions, 90 °C and 80% rH, by Zou et al.[42] The high value of R^2 indicated a degradation process that is mostly random over the whole aging period. Results indicated that the fastest degradation of cellulose occurred in the tideline but also that it proceeded faster in the area below than in the area above the tideline. It should be noted that these rates of glycosidic bond cleavage are for cellulose only and do not necessarily extend to other polysaccharides.[44]

4. Conclusion

This study established that a specific degradation occurs in paper when it is submitted to a "tideline experiment" during which a brown line is formed at the wet/dry boundary. The accrued presence of organic acids (formic and acetic) and hydroperoxides confirmed that the location-specific degradation is initially oxidative in nature. For the first time, it was shown that various types of hydroperoxides were present, water-soluble and non-water-soluble, most probably in part hydroperoxide functions attached to the anhydroglucose units of the cellulose chain. Hydrolysis reactions promoted during the accelerated aging at 100 °C and occurring at a given constant rate, which was calculated, have been evidenced to be more severe at the tideline than in any of the other areas of the paper. The reaction constant k, determined using the Ekamstam model for the degradation of linear polymers as the glycosidic bond breaking

Table 3. Number Average (M_n) and Weight Average (M_w) Molar Masses and Polydispersity (PDI) of Cellulose of Reference Whatman Paper No. 1 (ref), Cellulose in the Tideline (TL), above the Tideline (aTL), and below the Tideline (bTL)[a]

aging (h)	paper area	M_n (g mol^{-1}) ± RSD%	M_w (g mol^{-1}) ± RSD%	PDI (M_w/M_n)
0	ref	$3.96\times10^5\pm4.5\%$	$5.62\times10^5\pm2.1\%$	1.42
	aTL	$4.29\times10^5\pm2.7\%$	$5.71\times10^5\pm1.1\%$	1.33
	TL	$3.89\times10^5\pm1.9\%$	$5.47\times10^5\pm1.4\%$	1.41
	bTL	$4.23\times10^5\pm3.4\%$	$5.74\times10^5\pm0.5\%$	1.36
48	ref	$3.67\times10^5\pm3.3\%$	$4.93\times10^5\pm4.5\%$	1.34
	aTL	$3.56\times10^5\pm2.5\%$	$4.95\times10^5\pm2.3\%$	1.39
	TL	$2.85\times10^5\pm4.2\%$	$4.14\times10^5\pm1.6\%$	1.45
	bTL	$3.04\times10^5\pm3.5\%$	$4.41\times10^5\pm1.3\%$	1.45
120	ref	$2.74\times10^5\pm3.5\%$	$4.24\times10^5\pm2.1\%$	1.55
	aTL	$2.81\times10^5\pm2.0\%$	$4.05\times10^5\pm1.1\%$	1.44
	TL	$1.95\times10^5\pm2.4\%$	$3.11\times10^5\pm0.4\%$	1.60
	bTL	$2.30\times10^5\pm3.5\%$	$3.50\times10^5\pm1.8\%$	1.52

[a] Before and after accelerated aging in closed vessels at 100 °C for 48 and 120 h.

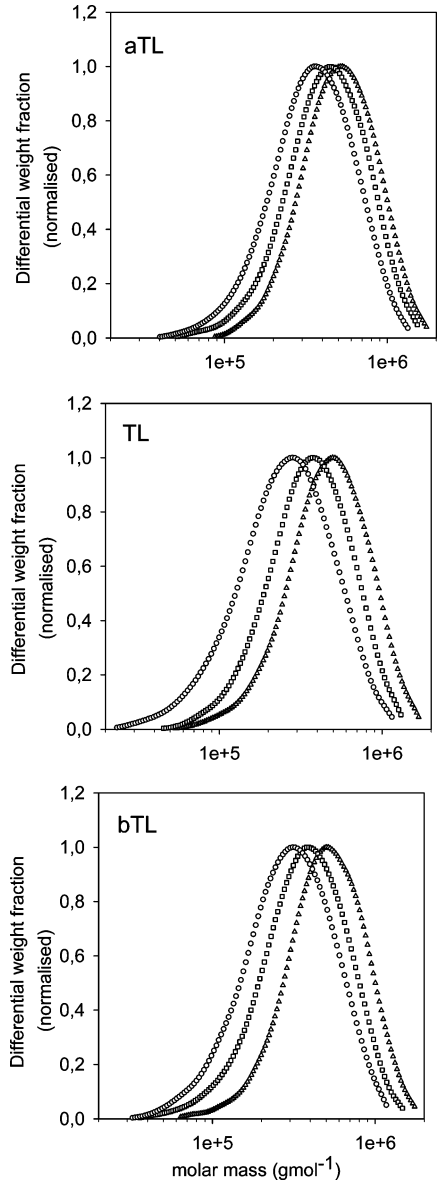

Figure 8. Overlay graphs of MMD of cellulose as a function of accelerated aging for each area (aTL, TL, and bTL) of unaged paper (Δ) and paper aged at 100 °C in closed vessel for 48 (□) and 120 h (○).

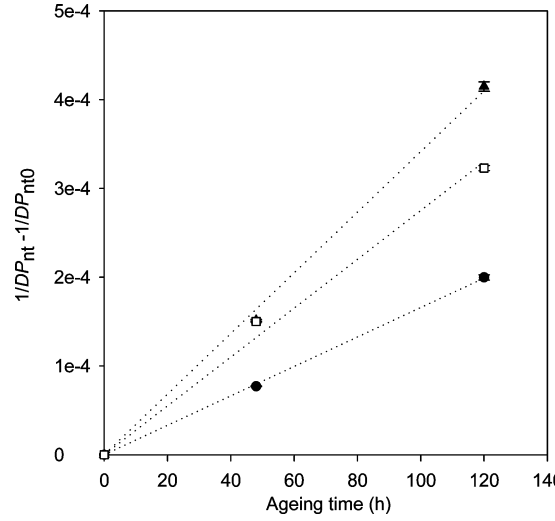

Figure 9. ($1/DP_{nt} - 1/DP_{nt0}$) of cellulose as a function of aging time (h) at 100 °C in closed vessels for each area of the paper, above the tideline (●), at the tideline (▲), and below the tideline (□).

rate for cellulose, was more than two times larger in the tideline than in the area above the tideline, the latter being similar to that of reference Whatman paper No.1. It is also noteworthy that the area that had undergone the passage of water, the area below the tideline, degraded faster than the area that had not been wetted during the experiment, the area above the tideline, the reaction constant k being about 1.6 times higher. Besides hydrolysis, accelerated aging led also to an overall increase in oxidation in all the areas of the paper, evidenced by elevated concentrations of acids and hydroperoxides. These findings have obvious implications for the local use of water and aqueous solutions on cellulosic materials, being it for usage issues or for mechanical property enhancement treatments, but particularly so for conservation treatments of cultural heritage objects.

Acknowledgment. The authors wish to thank Marie Schuler and Aude Izel for their help in the project during their internship at CRCC. We are grateful to Bertrand Lavédrine, director of CRCC, for scientific support of this research.

References and Notes

(1) Bone, W. H. *J. Soc. Dyers Colour.* **1934**, *50*, 307–309.
(2) Bone, W. H.; Turner, H. A. *J. Soc. Dyers Colour.* **1950**, *66*, 315–327.
(3) Bogaty, H.; Campbell, K. S.; Appel, W. D. *Text. Res. J.* **1952**, *22*, 75–81.
(4) Madaras, G. W.; Turner, H. A. *J. Soc. Dyers Colour.* **1953**, *69*, 371–377.
(5) Schaffer, R.; Appel, W. D.; Forziati, F. H. *J. Res. Natl. Inst. Stand. Technol.* **1955**, *54* (2), 103–106.
(6) Fox, M. R. *J. Soc. Dyers Colour.* **1965**, *81*, 7–11.
(7) Fox, M. R. *J. Soc. Dyers Colour.* **1965**, *81*, 46–51.
(8) Hutchins, J. K. *J. Am. Inst. Conserv.* **1983**, *22*, 57–61.
(9) Dupont, A.-L. *Restaurator* **1996**, *17*, 145–164.
(10) Dupont, A.-L. *Restaurator* **1996**, *17*, 1–21.

(11) Eusman, E. In *Conservation Research, Studies in the History of Art, Monograph Series II*, National Gallery of Art: Washington DC, 1995; Vol. 51, pp 11−27.
(12) Pedersoli, J. L.; Ligterink, F. *Restaurator* **2001**, *22*, 133–186.
(13) Bicchieri, M.; Ronconi, S.; Romano, F. P.; Pappalardo, L.; Corsi, M.; Cristoforetti, G.; Legnaioli, S.; Palleschi, V.; Salvetti, A.; Tognoni, E. *Spectrochim. Acta, Part B* **2002**, *57*, 1235–1249.
(14) Baynes-Cope, D. *Int. Biodeterior. Bull.* **1976**, *12*, 31–33.
(15) Press, R. E. *Int. Biodeterior. Biodegrad.* **2001**, *48*, 94–97.
(16) Ligterink, F. J.; Porck, H. J.; Smith, W. J. T. *The Paper Conservator* **1991**, *15*, 45–52.
(17) Dupont, A.-L.; Egasse, C.; Morin, A.; Vasseur, F. *Carbohydr. Polym.* **2007**, *68*, 1–16.
(18) Snyder, L. R., Kirkland, J. J., Glajch, J. L., Eds. In *Practical HPLC Method Development*, 2nd ed.; John Wiley & Sons, Inc.: New York, NY, 1997; p 695.
(19) Dupont, A.-L. *Polymer* **2003**, *44*, 4117–4126.
(20) Dupont, A.-L.; Harrison, G. *Carbohydr. Polym.* **2004**, *58*, 233–243.
(21) Röhrling, J.; Potthast, A.; Rosenau, T.; Lange, T.; Ebner, G.; Sixta, H.; Kosma, P. *Biomacromolecules* **2002**, *3*, 959–968.
(22) Striegel, A. M. *J. Chil. Chem. Soc.* **2003**, *48* (1), 73–77.
(23) Standard test method for accelerated temperature aging of printing and writing paper by dry oven exposure apparatus *D6819-02e02*; ASTM International: West Conshohocken, PA, 2002.
(24) Moisture in pulps, paper and paperboard. TAPPI test methods 1994−1995, Technical Association of the Pulp and Paper Industry *T 412 om-94*; TAPPI press: Atlanta, GA, 1994.
(25) Welf, E. S.; Venditti, R. A.; Hubbe, M. A.; Pawlak, J. J. *Prog. Pap. Recycl.* **2005**, *14* (3), 5–13.
(26) Orr, R. S.; Weiss, L. C.; Humphreys, G. C.; Mares, T.; Grant, J. N. *Text. Res. J.* **1954**, *24*, 399–406.
(27) du Plooy, A. B. J. *Appita* **1981**, *34* (3), 287–292.
(28) Dobarganes, M. C.; Velasco, J. *Eur. J. Lipid Sci. Technol.* **2002**, *104*, 420–428.
(29) Banerjee, D. K.; Budke, C. C. *Anal. Chem.* **1964**, *36* (4), 792–796.
(30) Gay, C.; Collins, J.; Gebicki, J. M. *Anal. Biochem.* **1999**, *273*, 149–155.
(31) Gebicki, J. M.; Guille, J. *Anal. Biochem.* **1989**, *176*, 360–364.
(32) Barnard, D.; Wong, K. C. *Anal. Chim. Acta* **1976**, *84*, 355–361.
(33) Denney, D. B.; Goodyear, W. F.; Goldstein, B. *J. Am. Chem. Soc.* **1960**, *82* (6), 1393–1395.
(34) Stein, R. A.; Slawson, V. *Anal. Chem.* **1963**, *35* (8), 1008–1010.
(35) Nakamura, T.; Maeda, H. *Lipids* **1991**, *26* (9), 765–768.
(36) Al-Malaika, S. In *Atmospheric Oxidation and Antioxidants*; Scott, G., Ed.; Elsevier: Amsterdam, 1993; p 48.
(37) Ott, E. , Spurlin, H. M., Grafflin, M. W. , Eds. In *Cellulose and Cellulose Derivatives*, 2nd ed.; Wiley: New York, NY, 1971.
(38) Fengel, D.; Wegener, G. In *Wood: Chemistry Ultrastructure, Reactions*; Walter de Gruyter: Berlin, Germany, 1984.
(39) Nevell, T. P. In *Cellulose Chemistry and its Applications*, Ellis Horwood Series Chemical Science; Nevell, T. P., Zeronian, S. H., Eds.; Wiley: New York, NY, 1985; p 221.
(40) Ekamstam, A. *Ber. Dtsch. Chem. Ges.* **1936**, *69A*, 553–559.
(41) Stephens, C. H.; Whitmore, P. W.; Morris, H. R.; Bier, M. E. *Biomacromolecules* **2008**, *9*, 1093–1099.
(42) Zou, X.; Gurnagul, N.; Uesaka, T.; Bouchard, J. *Polym. Degrad. Stab.* **1994**, *43*, 393–402.
(43) Emsley, A. M.; Heywood, R. *Cellulose* **1997**, *4*, 1–5.
(44) Striegel, A. M. *Biomacromolecules* **2007**, *8*, 3944–3949.

BM8006067